



THERMO-HYDRAULIC OPTIMIZATION OF SHELL AND EXTERNALLY FINNED TUBES HEAT EXCHANGER BY THE THERMAL EFFICIENCY METHOD AND SECOND LAW OF THERMODYNAMICS

 **Elcio Nogueira**

Department of Mechanic and Energy, State University of Rio de Janeiro,
Brazil.

Email: elcionogueira@hotmail.com



ABSTRACT

Article History

Received: 4 July 2022

Revised: 17 August 2022

Accepted: 2 September 2022

Published: 19 September 2022

Keywords

Externally finned tube
Second law of thermodynamic
Shell and tube heat exchanger
Theoretical analysis
Thermal effectiveness
Thermal efficiency.

The application aims to determine the thermal and hydraulic performance of externally finned, counter-flow, Shell, and Tube Heat Exchangers (STHE). The application refers to the cooling of machine oil flowing in the annular region, including non-spherical cylindrical nanoparticles of Boehmite Alumina. The oil inlet temperature is equal to 80 °C. Sea water is a coolant with an inlet temperature of 20°C. The main parameter in the optimization process is the number of finned tubes used for oil cooling. Another optimization factor is the number of heat exchanger units connected by hairpin. The number of fins per tube is fixed, equal to 34. The oil flow is set and equal to 4.0 kg/s. The inlet water flow varies, with a maximum flow of 5.0 kg/s. The quantities determined for analysis are: the thermal effectiveness, the actual and maximum heat transfer rates, the pressure drops caused in the tubes and by the flow in the annular region and fin system, the thermal and viscous irreversibilities, and the fluid outlet temperatures, and the thermodynamic Bejan number. It was determined that increasing the number of finned tubes from two to six tubes leads to better thermal and hydrodynamic performance. That is, it produces a favorable cost-benefit, to the detriment of the high viscous dissipation caused by the oil in the annular region. As an object of analysis, the inclusion of nanoparticles showed a significant improvement in thermal performance and an increase in viscous dissipation, with a slight decline in the Bejan number.

Contribution/Originality: The method of thermal efficiency of heat exchangers is a solution procedure that has recently been applied to various types of heat exchangers. When associated with viscous irreversibility and the thermodynamic Bejan number, it enables theoretical optimization analysis that can be helpful in the design and testing phase of heat exchangers. There are few academic works dealing with externally finned tube heat exchangers. The presented procedure is innovative as it includes them together to improve thermal performance and, at the same time, significantly reduce viscous dissipation. The use of nanoparticles amplify innovation.

1. INTRODUCTION

Finned tubes are widely used to passively improve heat transfer in circular tubes (one of the most used heat transfer surfaces in heat exchangers). Extended surfaces, called fins, are applicable when an additional area is needed to increase heat transfer. As far as the geometry of the fins is concerned, most of them are strips of metal with surfaces positioned longitudinally along the axis of the tube. Many experimental and numerical investigations

have been conducted on different types of tubes with internal fins using a variety of fluids (air, water, oil, ethylene, etc.). However, it is observed that literature is scarce regarding investigations in tubes with external fins.

Zafar, et al. [1] numerically investigate finned rings with longitudinal fins of the triangular cross-section. The work aims to obtain optimized configurations where the cost-benefit ratio can be as favourable as possible. They use the finite element method and genetic algorithm for configuration optimization. The results obtained provide optimal use of energy together with cost savings. Recommend the use of at least 18 fins.

Muhammad, et al. [2] numerically investigate numerous geometric configurations in a double tube heat exchanger with triangular fins. The use of the DG-FEM - Galerkin finite element method to explore the thermal characteristics of the arrangements in the thermal performance of the heat exchanger under analysis. They conclude, among others, that the Nusselt number increases with the values of the solid and fluid thermal conductivity ratio and suggest that the thermal resistance between the media plays a fundamental role in the design of the heat exchanger.

Ghazala, et al. [3] perform a numerical study using finite difference techniques in an externally finned shell and tube heat exchanger. They investigate the influence of variations in fin height, number of fins, and thermal conductivities on thermohydraulic performance and discuss optimal configurations. They make comparisons with results from the literature to validate the developed procedure. They conclude, among other things, that the height and the number of fins are the most effective geometric parameters.

Muhammad, et al. [4] propose an innovative diamond-shaped fin profile, which they claim to be the first work of its kind for a double finned tube heat exchanger. The designed profile allows automatic transformation, with changes of some parameters, in triangular and rectangular profiles available in the literature. They use the finite element technique to solve the problem. They present the most recommended shapes for the quantities associated with the fins, introducing variations in the height and width of the fins, both for thermal performance and viscous dissipation. They clarify that the recommendations are valid for the ratio between the radii of the inner and outer tubes, equal to 0.25.

Arvind and Yesyahu [5] state that the practical use of correlations to determine the thermal performance of finned tube heat exchangers is limited by the large number of parameters that can influence the Nusselt number and the friction factor. In this sense, they conclude, empirical correlations have many limitations in terms of applicability. They describe a methodology to evaluate the thermo-hydraulic performance of a finned tube heat exchanger with internal and external fins. Initially, they use the usual correlations for smooth tube flow and flat plate flow, which are numerically adjusted through successive substitutions. Then, they use correlations in the literature to prove the procedure performed when applied to simple cases. They observe that adding fins reduces the Nusselt number, but the heat transfer rate increases due to the rise in the total heat exchange area.

Górecki, et al. [6] elaborate on a tubular heat exchanger project composed of individually finned heat tubes and conduct an experimental study and mathematical modeling to develop a thermal model based on empirical correlations obtained from experimental work. Based on the "brute force" method, the global cost optimization process made it possible to determine the most suitable parameters for the heat exchanger under analysis. The mathematical modeling results produced a good agreement with experimental results, with a maximum relative difference equal to 10%.

Prottay, et al. [7] perform a performance study of double tube heat exchangers connected by a clamp (hairpin) for oil cooling. This work aims to obtain geometric parameters that optimize the configuration under analysis for a better cost-benefit relationship between heat exchange and pressure drop observed in the heat exchanger since the pressure drop impacts the energy per unit of time generated by the pumping system.

Shiva and Murthy [8] analyze the performance of concentric tube heat exchangers using by passive heat transfer technique. They use different longitudinal profiles of fins: rectangular, parabolic, and triangular. For performance analysis, the mass flows of the internal and external fluids vary, keeping the base and height of the fin

constant. They conclude that the fin system allows a higher heat transfer rate concerning the non-finned tube, with higher rates for the configuration with a rectangular profile fin.

Ayon, et al. [9] designed a compact shell and tube heat exchanger to obtain high thermal efficiency and minimum cost. The heat exchanger under analysis contains inner tubes with axes parallel to the shell to cool oil using seawater. They report that limits were established for the difference in fluid outlet temperatures and total pressure drop as fundamental parameters for minimizing cost and maximizing thermal effectiveness.

Heidar, et al. [10] analyze a radial finned shell and tube heat exchanger, using nine physical parameters as a reference. The main parameters used for analysis are tube diameter, length, number of tubes, and fins. They determine the coefficients related to heat transfer and pressure drop on the hull side using the "modified Delaware" technique. They obtain an optimal compromise between heat transfer rate, ranging from 3517 to 7075 kW, and pipe pressure drop, ranging from 3.8 to 46.7 kPa.

Faraz, et al. [11] use nanoparticles in different volumetric concentrations to numerically analyze the thermal performance of a shell and finned tube heat exchangers. They use Fe₂O₃ nanoparticles in water as a base fluid at concentrations of 1.0%, 1.5%, and 2.0%. They use ANSYS Fluent software for numerical simulation and comparison with results obtained for pure water. They report that increasing the proportion of nanoparticles causes greater thermal efficiency without significant pressure drop and that a volumetric fraction equal to 2.0 % allows an increase of 19.1% in the heat transfer rate.

Nogueira [12] uses concepts of efficiency and thermal effectiveness in thermal analysis of shell and tube condenser using Freon 134a as refrigerant flowing in the shell. The analysis includes three conditions for the coolant along the hull: superheated steam, saturated steam, and saturated liquid. Each of the three regions contains four tubes, consisting of 12 tubes. Horizontal flow deflectors are included in the superheated steam region. Temperature, efficiency, and effectiveness profiles were obtained for the three regions under analysis, with water-based aluminum oxide nanoparticles flowing in the tubes. The refrigerant flow rate is fixed, equal to 0.20 kg/s, and the nanofluid flow rate varies from 0.05 kg/s to 0.40 kg/s. It performs a comparative analysis with experimental results obtained in the literature for steam pressure equal to 1.2 Mpa and water flow equal to 0.41 kg/s.

Nogueira [13] applies the second law of thermodynamics through the concepts of efficiency, effectiveness, and thermal irreversibility to analyze shell and tube, heat exchangers. Water flows in the hull with an inlet temperature of 27°C, and a water-ethylene glycol mixture with volume fractions of silver nanoparticles (Ag) or aluminum dioxide (Al₂O₃) flows in the tube with an inlet temperature of 90°C. The water flow rate in the shell is kept constant, equal to 0.23 kg/s, and the flow of 50% ethylene glycol varies from 0.01 to 0.50 kg/s. Results were obtained graphically, changing the volume fraction for the nanoparticles. It is shown that the flow regime has a significant effect on the performance of the heat exchanger.

2. METHODOLOGY

It analyzes configurations of heat exchangers with finned inner tubes, as shown in Figure 1. Figure 2 shows shell and tube heat exchangers connected through a clamp. This type of configuration, called hairpin in the literature, is used to optimize the space where heat exchangers will be installed.

Table 1 presents the properties of the oil, water, and Alumina. For performance analysis, the non-spherical cylindrical Alumina nanoparticles, with a volume fraction equal to 5.0%, will be associated with the oil.

Table 1. Thermodynamic properties of hot and cold fluids and boehmite alumina.

	ρ kg/m ³	k W/(m K)	C_p J/(kg K)	μ kg/(m s)	ν m ² /s	α m ² /s	Pr
Oil (hot)	885.27	0.1442	1902	$7.5 \cdot 10^{-2}$	$8.47 \cdot 10^{-5}$	$8.56 \cdot 10^{-8}$	989
Water (cold)	1013.4	0.639	4004	$9.61 \cdot 10^{-4}$	$9.48 \cdot 10^{-7}$	$1.57 \cdot 10^{-7}$	6.02
B. Alumina	3050	30.0	618.3	-	-	-	-

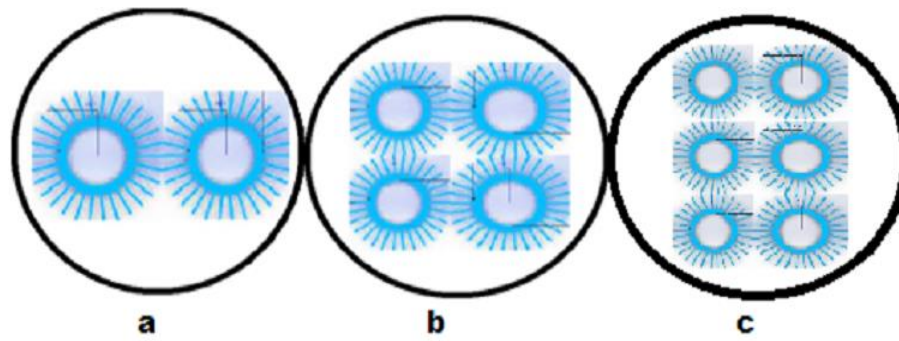


Figure 1. Shell and externally finned tubes with rectangular fins [7].

a – 2 finned tubes; b – 4 finned tubes; c – 6 finned tubes.

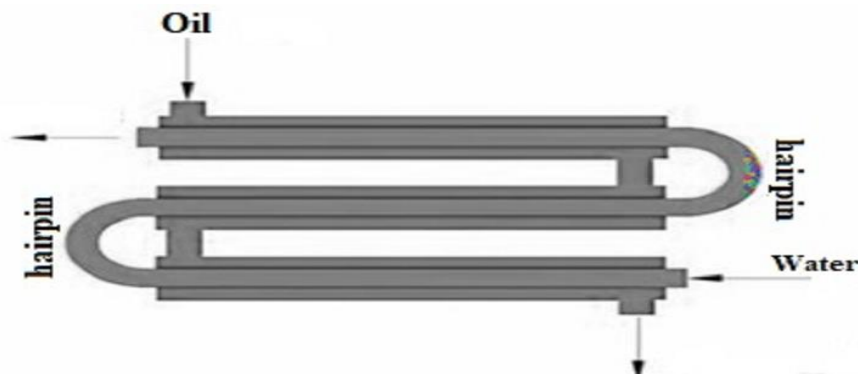


Figure 2. Shell and Tube Exchangers in counter flow and connected through hairpin.

The formulation, with the data necessary to determine the quantities of interest in the analysis, is described below.

$$Th_i = 80^\circ C \quad (1)$$

$$Tc_i = 20^\circ C \quad (2)$$

Equations 1 and 2 represented by Th_i and Tc_i are the inlet temperatures of the hot and cold fluids, respectively.

$$NHE = 2 \text{ standard value}; 1 \leq NHE \leq 4 \quad (3)$$

Equation 3 represented by NHE is the number of heat exchangers connected by hairpin and considered for analysis.

$$N_{Tube} = 2 \text{ standard value} \quad (4)$$

Equation 4 represented by N_{Tube} is the number of finned tubes per heat exchanger unit.

$$L_{Tube} = 4.0 \text{ m} \quad (5)$$

Equation 5 represented by L_{Tube} is the length of each heat exchanger unit.

$$L_{Total} = NHE L_{Tube} \text{ m} \quad (6)$$

Equation 6 represented by L_{Total} is the total length considered for the heat exchange.

$$H_{Fin} = 1.2710^{-2} \text{ m} \quad (7)$$

$$\Delta_{Fin} = 9.010^{-4} \text{ m} \quad (8)$$

$$N_{Fin} = 34 \quad (9)$$

Equations 8 and 9 represented by Δ_{Fin} and N_{Fin} are the fin thickness and the number of fins per tube.

$$k_w = 52.0 \text{ W / (mK)} \quad (10)$$

Equation 10 represented by k_w is the thermal conductivity of the fin material.

$$Dc_i = 0.254 \text{ m} \quad (11)$$

$$Dc_o = 0.27432 \text{ m} \quad (12)$$

Equations 11 and 12 represented by Dc_i and Dc_o are the inner and outer diameters of the tubes.

$$Dh_i = 0.3957 \text{ m for two finned tubes} \quad (13a)$$

$$Dh_i = 0.5563 \text{ m for four finned tubes} \quad (13b)$$

$$Dh_i = 0.67564 \text{ m for six finned tubes} \quad (13c)$$

Equations 13 represented by Dh_i is the inner diameter of the shell.

$$A_c = \frac{\pi Dc_i^2}{4} \text{ m}^2 \quad (14)$$

Equation 14 represented by A_c is the cross-sectional area for internal flow in the tube.

$$Dh_c = Dc_i \quad (15)$$

$$De_c = Dc_i \quad (16)$$

Equations 15 and 16 represented by Dh_c and De_c are the hydraulic and equivalent diameters for the tubes.

$$A_h = \frac{\pi Dh_i^2 - N_{Tube} \pi Dc_o^2}{4} - N_{Tube} N_{Fin} H_{Fin} \Delta_{Fin} \quad (17)$$

Equation 17 represented by A_h is the cross-sectional area for flow outside the tubes.

$$Ph_w = \pi Dh_i - N_{Tube} \pi Dc_o + 2H_{Fin} N_{Fin} N_{Tube} \quad (18)$$

$$Ph_h = N_{Tube} \pi Dc_o + 2H_{Fin} N_{Fin} N_{Tube} \quad (19)$$

$$Dh_h = \frac{4A_h}{Ph_w} \quad (20)$$

$$Dh_e = \frac{4A_h}{Ph_h} \quad (21)$$

Equations 20 and 21 represented by Dh_h and Dh_e are the hydraulic and equivalent diameters associated with the annular region.

$$A_{Total} = \pi Dc_o L_{Tube} N_{Tube} + 2(H_{Fin} L_{Tube} + H_{Fin} \Delta_{Fin}) N_{Fin} N_{Tube} \quad (22)$$

Equation 22 represented by A_{Total} is the heat transfer area for the configurations under analysis.

For the compound oil + Boehmite Alumina Nanoparticles, we have Monfared, et al. [14]:

$$\mu_h = \mu_h (1 + A_1 \phi + A_2 \phi^2) \quad (23)$$

$$k_h = k_h (1 + C_k \phi) \quad (24)$$

Equation 24 represented by ϕ is the volume fraction of Boehmite Alumina Nanoparticles. $A_1 = 37.1$, $A_2 = 904.4$ and $C_k = 2.61$ are constants associated with cylindrical non-spherical nanoparticles [14].

$$\rho_h = \rho_{Al} \phi + (1 - \phi) \rho_h \quad (25)$$

$$Cp_h = \frac{(1 - \phi) \rho_h Cp_h + \rho_{Al} Cp_{Al} \phi}{\rho_h} \quad (26)$$

$$v_h = \frac{\rho_h}{\mu_h} \quad (27)$$

$$\alpha_h = \frac{k_h}{\rho_h Cp_h} \quad (28)$$

$$V_c = \frac{(\dot{m}_c / N_{Tube})}{\rho_c A_c} \quad (29)$$

$$V_h = \frac{\dot{m}_h}{\rho_h A_h} \quad (30)$$

$$\text{Re}_c = \frac{\rho_c V_c Dh_c}{\mu_c} \quad (31)$$

$$\text{Re}_h = \frac{\rho_h V_h Dh_h}{\mu_h} \quad (32)$$

Re_c and Re_h are the Reynolds numbers associated with the cold and hot fluids.

$$\text{Nu}_c = 0.023 \text{Re}_c^{0.8} \text{Pr}_c^{0.4} \quad (33)$$

$$\text{Nu}_h = 1.86 \left(\frac{\text{Re}_h \text{Pr}_h Dh_e}{L_{\text{Tube}}} \right)^{(1/3)} \left(\frac{\mu_h}{\mu_w} \right)^{0.14} \quad (34)$$

Equations 33 and 34 represented by Nu_c and Nu_h are the Nusselt numbers associated with the cold and hot fluids, respectively. $\mu_w = 19.410^{-2} \text{ kg / (ms)}$ is the absolute viscosity near the surface that exchanges heat with the fluid.

$$h_c = \frac{\text{Nu}_c k_c}{De_c} \frac{W}{(m^2 K)} \quad (35)$$

$$h_h = \frac{\text{Nu}_h k_h}{Dh_e} \frac{W}{(m^2 K)} \quad (36)$$

$$\text{Rf}_c = 8.810^{-5} \frac{m^2 K}{W} \quad (37)$$

$$\text{Rf}_h = 1.710^{-4} \frac{m^2 K}{W} \quad (38)$$

Equations 37 and 38 represented by Rf_c and Rf_h are the fouling factors for water and oil, respectively.

$$mL = \sqrt{\frac{2h_h}{\Delta_{Fin} k_w}} \frac{1}{m} \quad (39)$$

$$\eta_{Fin} = \frac{\text{Tanh}(mLH_{Fin})}{mLH_{Fin}} \quad (40)$$

Equation 40 represented by η_{Fin} is the efficiency associated with the fin.

$$\eta'_{Fin} = 1 - (1 - \eta_{Fin}) \frac{2(H_{Fin} L_{Tube} + H_{Fin} \Delta_{Fin}) N_{Fin} N_{Tube}}{A_{Total}} \quad (41)$$

$$U_o = \frac{1}{\frac{1}{h_c} + Rf_c + \frac{1}{\eta_{Fin} h_h} + Rf_h} \quad (42)$$

Equation 42 represented by U_o is the overall heat transfer coefficient.

$$C_c = \dot{m}_c C_{p_c} \quad (43)$$

$$C_h = \dot{m}_h C_{p_h} \quad (44)$$

$$C^* = \frac{C_{\min}}{C_{\max}} \quad (45)$$

Equations 43 and 44 represented by C_c and C_h are the heat capacities associated with cold and hot fluids.

C_{\min} is the smallest of the heat capacities.

$$NTU = \frac{U_o A_{Total}}{C_{\min}} \quad (46)$$

Equation 46 represented by NTU is the number of thermal units associated with the configuration under analysis.

$$Fa = \frac{NTU}{2} (1 - C^*) \quad (47)$$

$$\eta_T = \frac{\tanh(Fa)}{Fa} \quad (48)$$

Equation 48 represented by η_T is the thermal efficiency of the heat exchanger [15].

$$\varepsilon_T = \frac{1}{\frac{1}{\eta_T NTU} + \frac{1 + C^*}{2}} \quad (49)$$

Equation 49 represented by ε_T is the thermal effectiveness associated with the configuration under analysis.

$$\dot{Q} = \varepsilon_T C_{\min} (Th_i - Tc_i) \quad (50)$$

$$\dot{Q}_{\max} = C_{\min} (Th_i - Tc_i) \quad (51)$$

Equation 50 represented by \dot{Q} is the heat transfer rate associated with the configuration under analysis.

$$Th_o = Th_i - \frac{\dot{Q}}{C_h} \quad (52)$$

$$Tc_o = Tc_i + \frac{\dot{Q}}{C_c} \quad (53)$$

Equation 53 represented by Th_o and Tc_o are the outlet temperatures of the hot and cold fluids, respectively.

$$\sigma_T = \frac{C_h}{C_{\min}} \ln\left(\frac{Th_o}{Th_i}\right) + \frac{C_c}{C_{\min}} \ln\left(\frac{Tc_o}{Tc_i}\right) \quad (54)$$

$$\dot{S}_{genT} = \sigma_T C_{\min} \quad (55)$$

Equations 54 and 55 represented σ_T and \dot{S}_{genT} are the thermal irreversibility and the thermal entropy generation rate.

$$f_h = \exp(0.567 - 0.19 \text{Re}_h) \quad (56)$$

$$\Delta P_h = N_{Tube} f_h \left(\frac{L_{Tube}}{Dh_i}\right) \left(\frac{\rho_h V_h^2}{2}\right) \quad (57)$$

Equation 56 represented by f_h is the friction factor in the annular region. ΔP_h is the pressure drop in the annular region.

$$D_{hFin} = Dh_i - Dc_o \quad (58)$$

$$\text{Re}_{hFin} = \frac{\rho_h V_h D_{hFin}}{\mu_h} \quad (59)$$

$$f_{hFin} = 0.646 \text{Re}_{hFin}^{(-0.5)} \quad (60)$$

$$\Delta P_{hFin} = f_{hFin} \left(\frac{\rho_h V_h^2}{2}\right) \frac{L_{Tube} N_{Tube} (H_{Fin} + \Delta_{Fin})}{H_{Fin}^2} \quad (61)$$

Equation 61 represented by ΔP_{hFin} is the pressure drop associated with the set of fins of the configuration under analysis.

$$f_c = \frac{0.316}{\text{Re}_c^{0.25}} \quad (62)$$

$$\Delta P_c = N_{Tube} f_c \left(\frac{L_{Tube}}{Dc_i}\right) \left(\frac{\rho_c V_c^2}{2}\right) \quad (63)$$

$$P_{Atm} = 101.325 \text{ Pa} \quad (64)$$

$$P_{2c} = P_{Atm} \quad (65)$$

$$P_{2h} = P_{Atm} \quad (66)$$

Equations 65 and 66 represented P_{2c} and P_{2h} are the outlet pressures of the cold and hot fluids.

$$P_{1c} = P_{2c} + \Delta P_c \quad (67)$$

$$P_{1h} = P_{2h} + \Delta P_h + \Delta P_{hFin} \quad (68)$$

$$R = \frac{Th_i - Th_o}{Tc_o - Tc_i} \quad (69)$$

$$\sigma_V = -\frac{C_h}{C_{min}} R \ln\left(\frac{P_{2h}}{P_{1h}}\right) - \frac{C_c}{C_{min}} R \ln\left(\frac{P_{2c}}{P_{1c}}\right) \quad (70)$$

$$\dot{S}_{genV} = \sigma_V C_{min} \quad (71)$$

Equations 70 and 71 represented σ_V and \dot{S}_{genV} are the viscous irreversibility and the viscous entropy generation rate.

$$Be = \frac{\dot{S}_{genT}}{\dot{S}_{genT} + \dot{S}_{genV}} \quad (72)$$

Equation 72 represented by Be is the Bejan thermodynamic number [16].

3. RESULTS AND DISCUSSION

The application refers to the cooling of machine oil flowing in the annular region, including non-spherical cylindrical nanoparticles of Boehmite Alumina. The oil inlet temperature is equal to 80 °C. Sea water is a coolant with an inlet temperature of 20°C. The main parameter in the optimization process is the number of finned tubes used for oil cooling. Another optimization factor is the number of heat exchanger units connected by hairpin. The number of fins per tube is fixed, equal to 34. The oil flow is fixed and equal to 4.0 kg/s. The inlet water flow varies, with a maximum flow of 5.0 kg/s.

Figures 3 - 5 present thermal effectiveness for three typical situations under analysis: 2, 4, and 6 finned tubes. The number of heat exchangers connected per clamp also varies, from 1 heat exchanger to 4 heat exchangers. The thermal effectiveness increases with the mass flow of water in the tubes, represented by the Reynolds number (Rec), with the number of finned tubes and the number of heat exchangers connected to each other.

The thermal effectiveness increases as the heat exchange area increase with the number of finned tubes. The effectiveness reaches maximum values of approximately 0.6, 0.8, and 0.9 for 2, 4 and 6 finned tubes, respectively Figures 3 - 5, when the number of connected heat exchangers equals 4. The Reynolds number for the refrigerant decreases with the number of finned tubes, because the total flow of water entering the heat exchanger is divided between the tubes. The thermal effectiveness is influenced by the volume fraction of the non-spherical cylindrical alumina nanoparticles, presenting higher values than those obtained for pure oil.

As the thermal effectiveness reflects the heat transfer rate value, the ratio between the actual heat transfer rate and the maximum heat transfer rate, the conclusions regarding the thermal effectiveness observed for 2, 4, and 6 finned tubes Figures 3-4, are valid for heat transfer rates Figures 6 - 8. Therefore, the predominant factor for

presenting these data is that the absolute numerical energy values per unit of time transferred between the fluids can be measured.

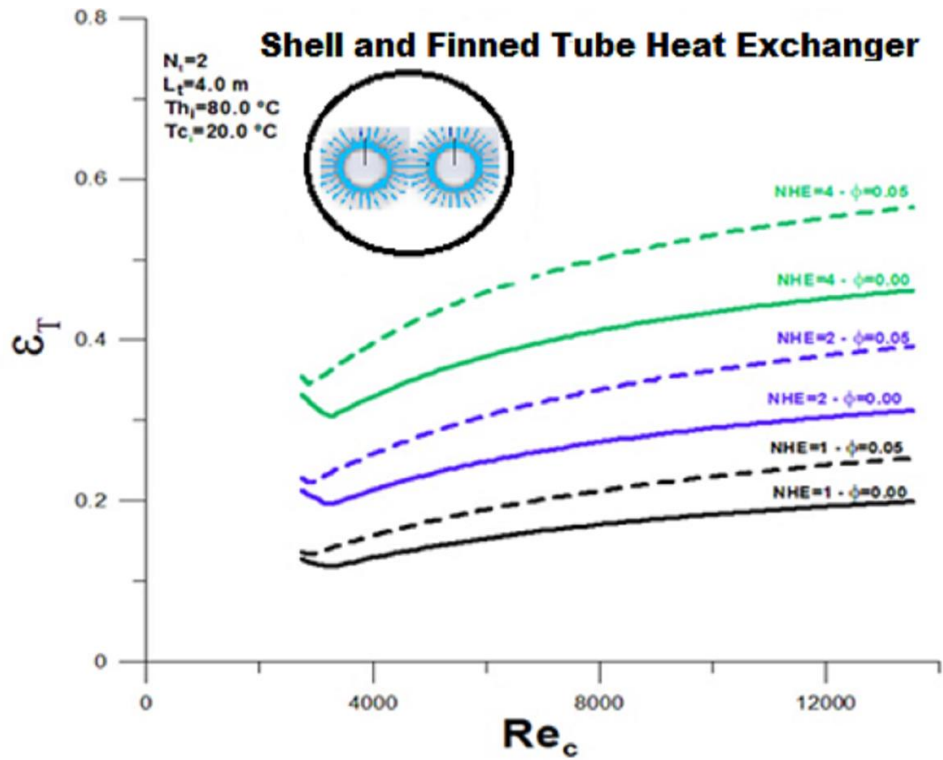


Figure 3. Thermal effectiveness for number of finned tubes equal to 2.

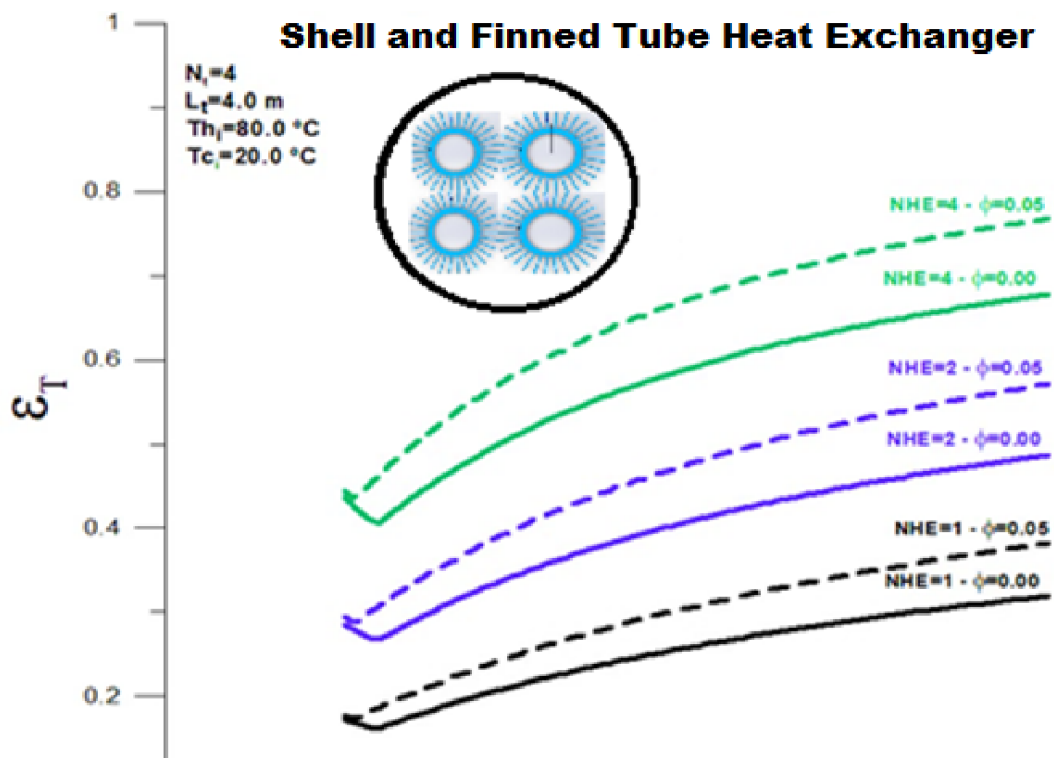


Figure 4. Thermal effectiveness for number of finned tubes equal to 4.

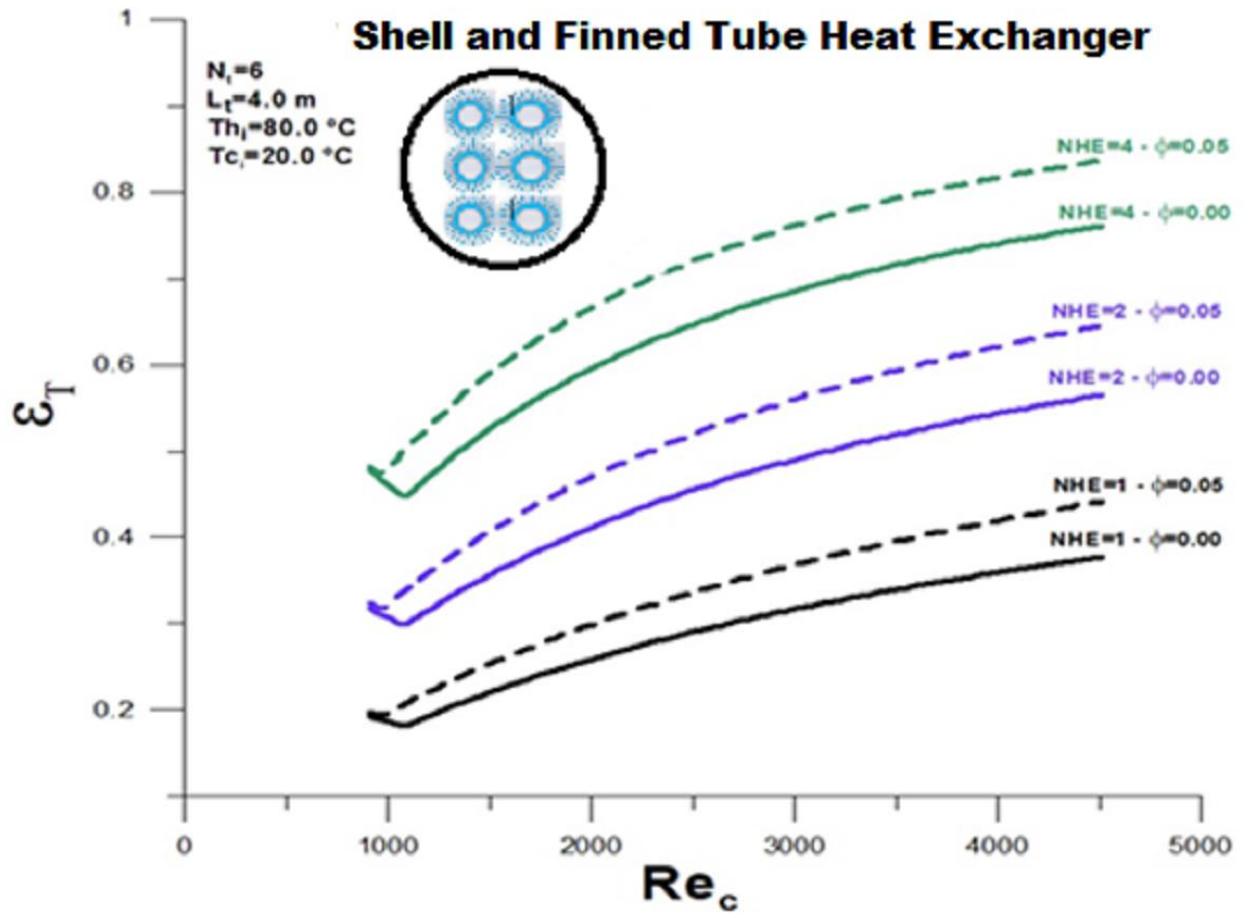


Figure 5. Thermal effectiveness for number of finned tubes equal to 6.

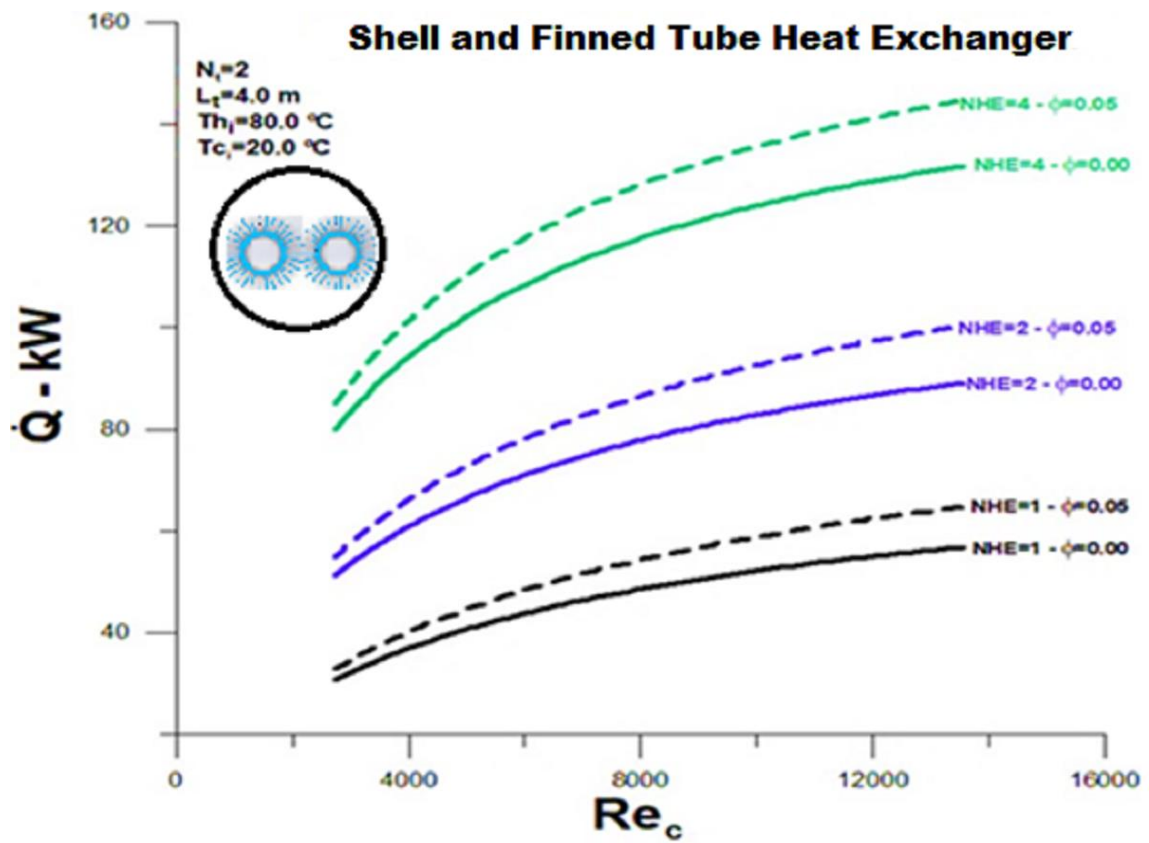


Figure 6. Heat transfer rate for number of finned tubes equal to 2.

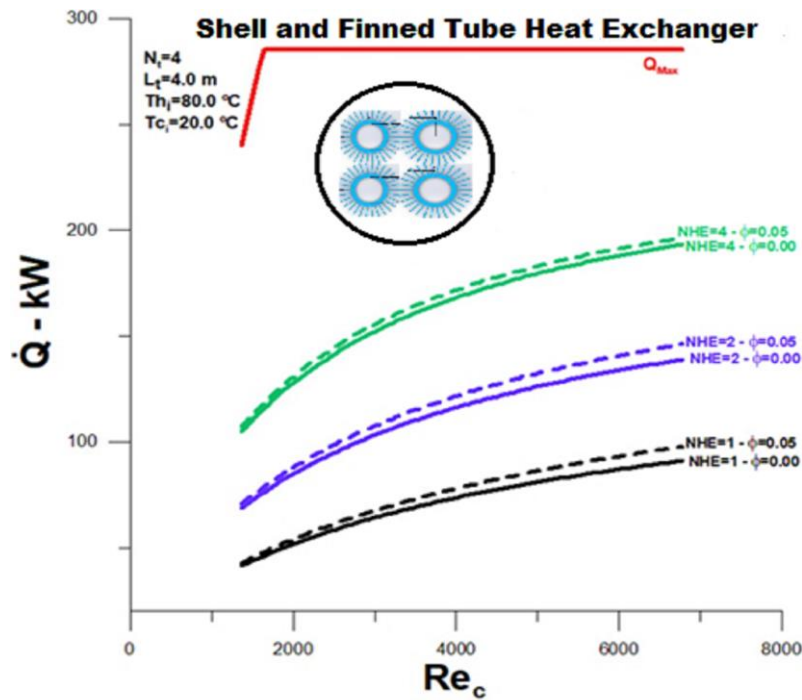


Figure 7. Heat transfer rate for number of finned tubes equal to 4.

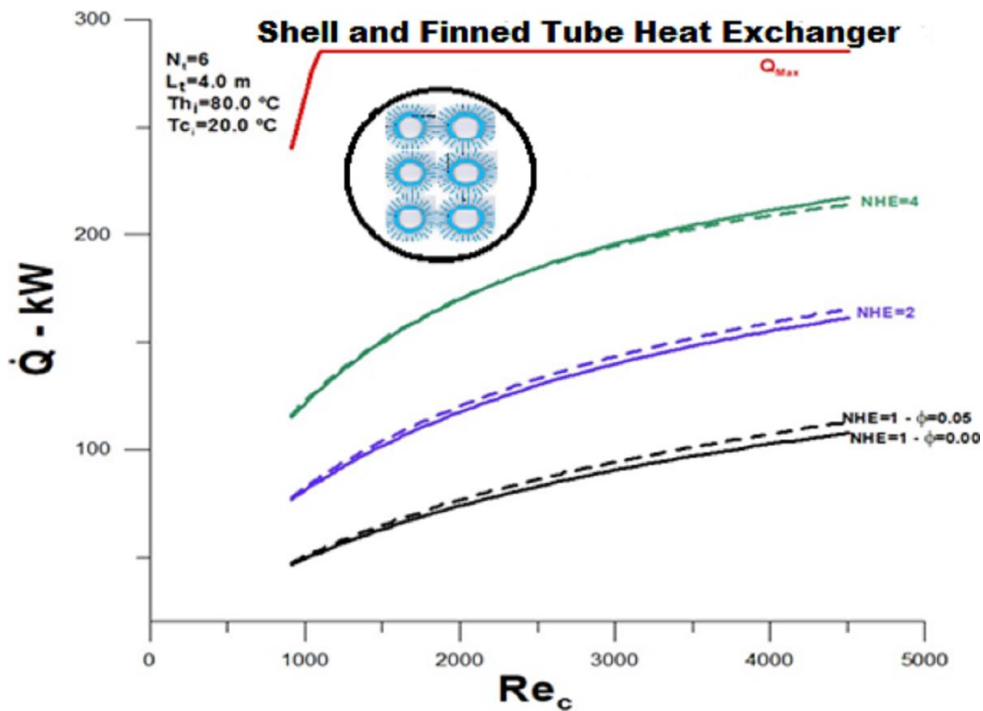


Figure 8. Heat transfer rate for number of finned tubes equal to 6.

The principal thermal quantity to measure the heat exchanger's actual thermal performance is, of course, the outlet temperature of the fluid to be cooled, a parameter presented in Figures 9 and 10.

Figure 9 shows the oil outlet temperature for some finned tubes equal to 2, 4, and 6, and two (NHE=2) clamp-connected heat exchangers. Again, one can observe the influence of non-spherical cylindrical alumina nanoparticles. For $N_t = 2$, the minimum temperature observed for pure oil is close to 62 °C; for oil, with a volume fraction of nanoparticles equal to 5.0%, the minimum temperature is close to 57 °C. In this last situation, using nanoparticles, there is a maximum gain of approximately 8.0% for thermal performance within the flow rate under analysis. For

$N_t = 4$, the minimum temperature observed for pure oil is close to 50 °C; for oil with a volume fraction of nanoparticles equal to 5.0%, the minimum temperature is close to 45 °C. In this last situation, using nanoparticles, there is a maximum gain of approximately 10.0% for thermal performance within the flow rate under analysis. For $N_t = 6$, the minimum temperature observed for pure oil is close to 46 °C. For oil with a volume fraction of nanoparticles equal to 5.0%, the minimum temperature is close to 41 °C. In this last situation, using nanoparticles, there is a maximum gain of approximately 11.0% for thermal performance within the flow rate under analysis.

Figure 10 shows the oil outlet temperature for a few finned tubes equal to 2,4, and 6 for four (NHE=4) clamp-connected heat exchangers. Again, one can observe the influence of non-spherical cylindrical alumina nanoparticles. For $N_t = 2$, the minimum temperature observed for pure oil is close to 54 °C; for oil with a volume fraction of nanoparticles equal to 5.0%, the minimum temperature is close to 48 °C. In this last situation, using nanoparticles, there is an approximate maximum gain of 11.1% for thermal performance within the flow rate under analysis. For $N_t = 4$, the minimum temperature observed for pure oil is close to 40 °C; for oil, with a volume fraction of nanoparticles equal to 5.0%, the minimum temperature is close to 34 °C. In this last situation, using nanoparticles, there is a maximum gain of approximately 15.0% for thermal performance within the flow rate under analysis. For $N_t = 6$, the minimum temperature observed for pure oil is close to 34 °C, and for oil with a volume fraction of nanoparticles equal to 5.0%, the minimum temperature is close to 29 °C. In this last situation, using nanoparticles, there is a maximum gain of approximately 15.0% for thermal performance within the flow rate under analysis.

The numbers demonstrate that the doubling of finned tubes brings a significant gain in thermal performance. When added by doubling the number of heat exchangers, the thermal performance is increased to approximately 24% when pure oil. And 29% with the introduction of nanoparticles. However, the gain with doubling the heat exchangers is significantly more significant than including nanoparticles with a 5.0% volume fraction for the same number of finned tubes.

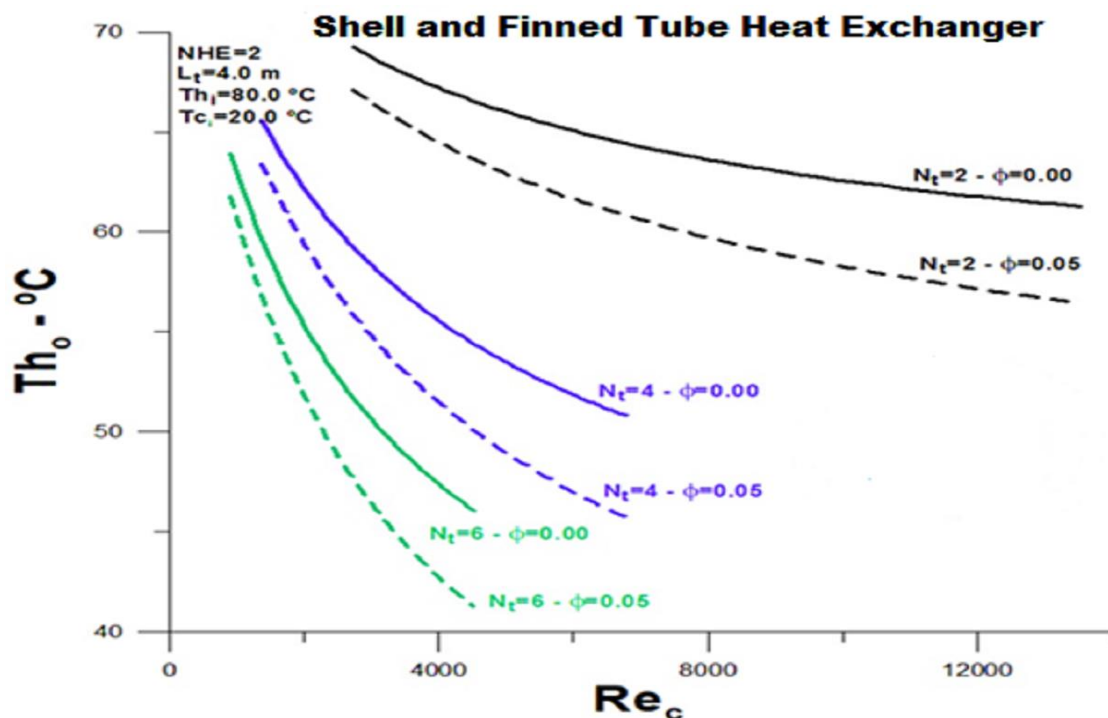


Figure 9. Oil outlet temperature for number of heat exchangers equal to 2.

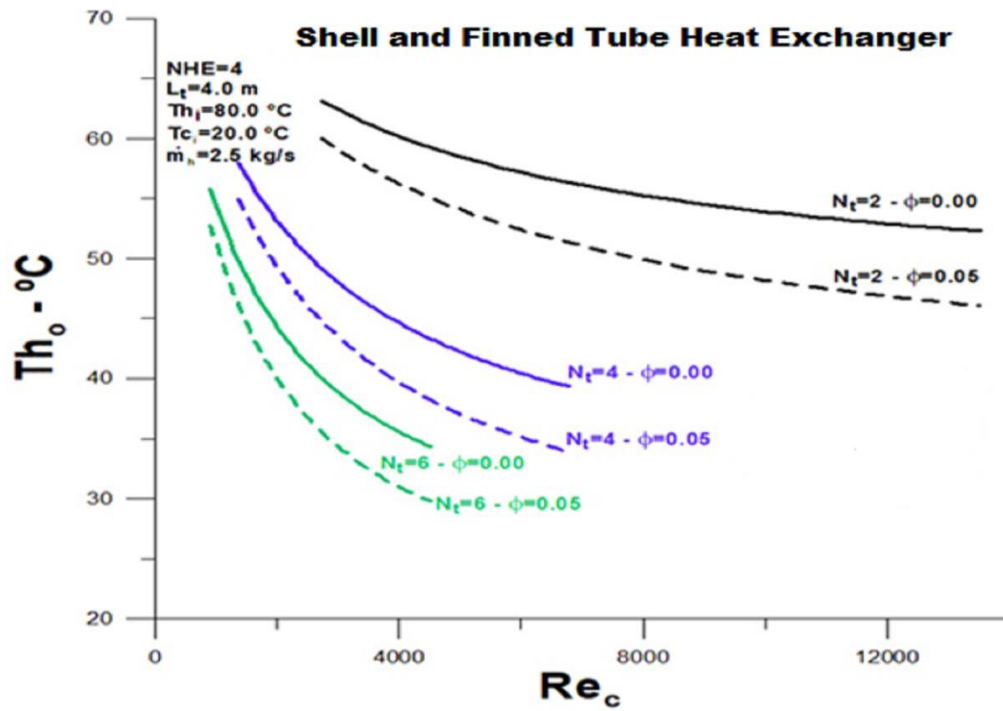


Figure 10. Oil outlet temperature for number of heat exchangers equal to 4.

Thermal irreversibility, Figures 11 - 13, are relevant factors for analyzing the global, systemic performance of the heat exchanger. Thermal irreversibility is, by nature, associated with thermal effectiveness and heat transfer rate since it represents the relative increase in the total entropy rate in thermal energy generation. As the objective when designing a heat exchanger is to obtain the best possible heat transfer between the fluids, despite the viscous irreversibility, the increase in thermal irreversibility tends to improve the performance of the heat exchanger in general. In this case, when observing the results presented in Figures 11 - 13, it is evident that the increase in the number of finned tubes points to an improvement in the overall performance of the heat exchanger. Analyzing the thermal performance with NHE ranging from 1 to 4, a gain of 50% is observed for $N_t=2$, 37% for $N_t=4$, and 32% for $N_t=6.0$.

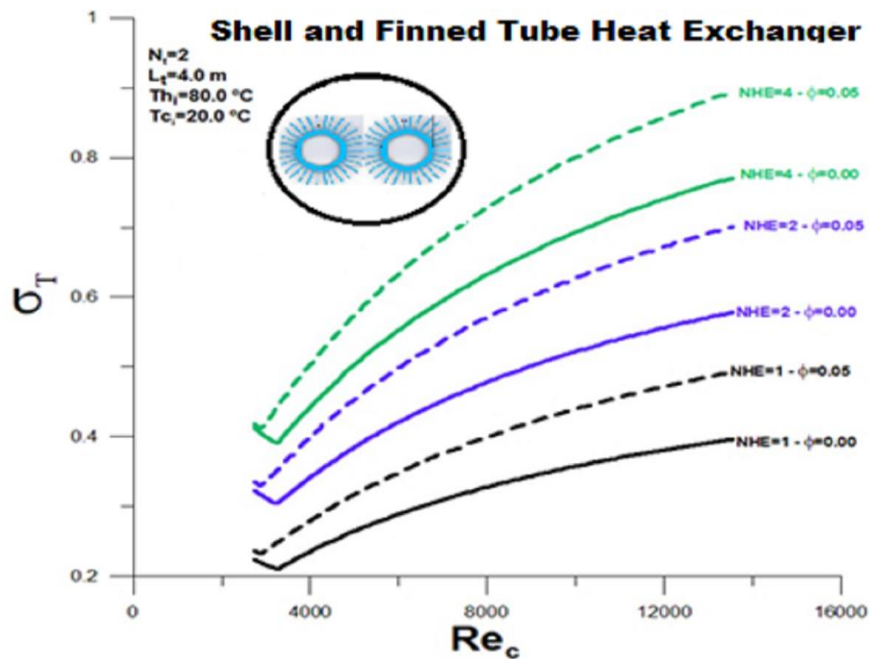


Figure 11. Thermal irreversibility for number of finned tubes equal to 2.

To analyze the overall performance of the heat exchanger, Figure 14 shows the total pressure drop in the annular region, where the fins are located. The pressure drop in the annular region is prevalent against the pressure drop in the tubes. The analysis encompasses the number of heat exchangers, the number of finned tubes, and alumina nanoparticles' influence. The pressure drop grows with the increasing number of heat exchangers and nanoparticle volume fraction. The most relevant is that the pressure drop decreases significantly when the number of finned tubes increases. This decrease is related to the relative increase in area for oil flow. This result is highly relevant to the system's overall performance under analysis regarding cost-benefit.

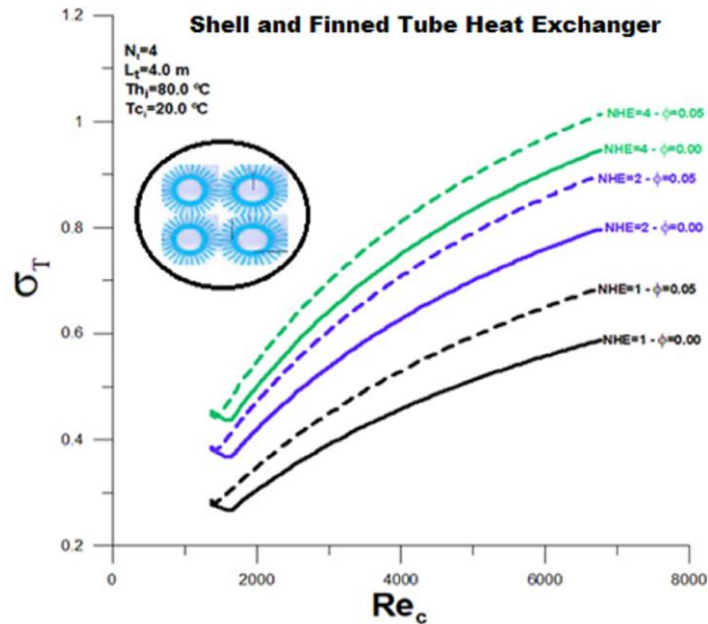


Figure 12. Thermal irreversibility for number of finned tubes equal to 4.

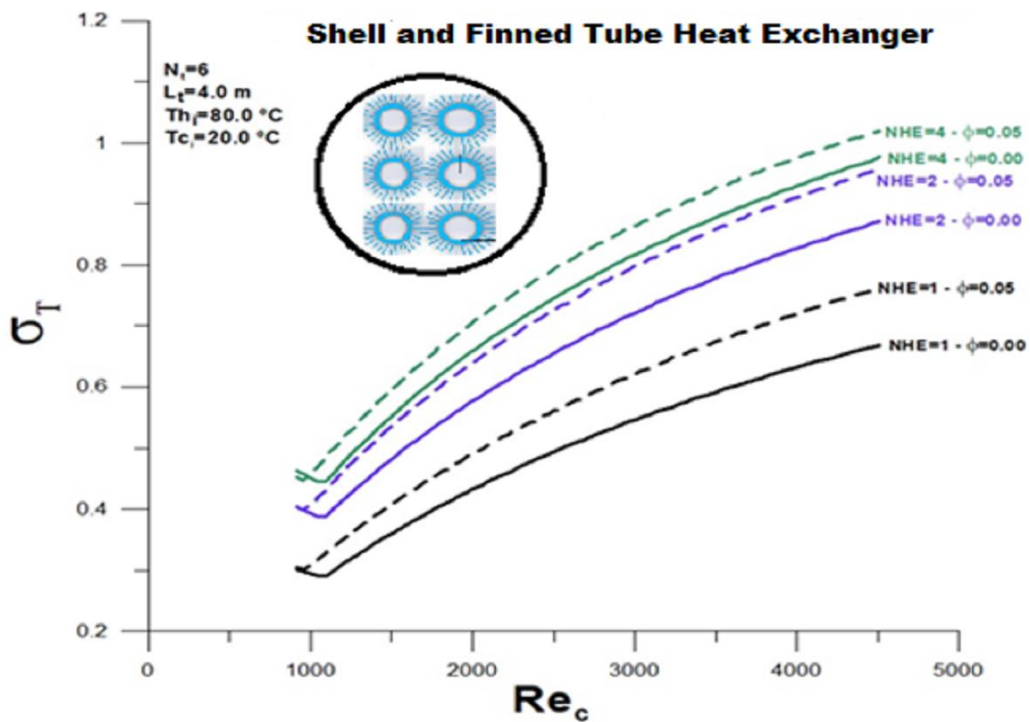


Figure 13. Thermal irreversibility for number of finned tubes equal to 6.

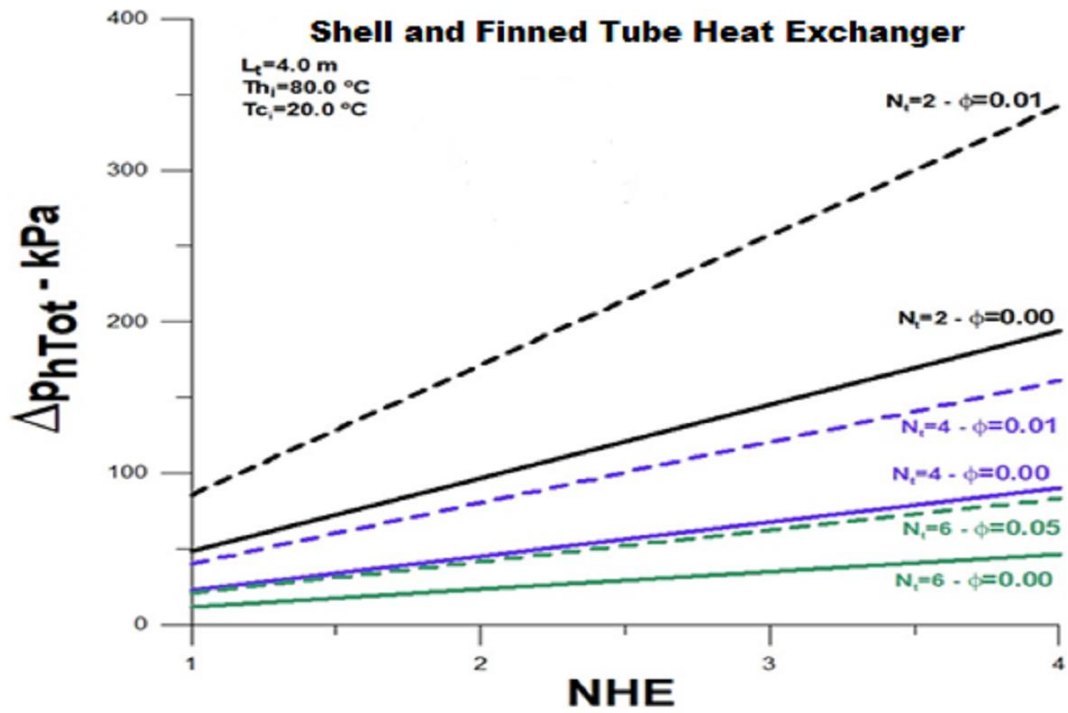


Figure 14. Total pressure drop in the annular region of the heat exchanger.

Figures 15 - 17 present results for viscous irreversibility for finned tube numbers equal to 2, 4 and 6, respectively.

Viscous irreversibility follows the trend of pressure drop since it is influenced by it. It is observed that the viscous irreversibility increases with the number of heat exchangers and decreases with the number of tubes since the expansion of finned tubes increases the oil passage area.

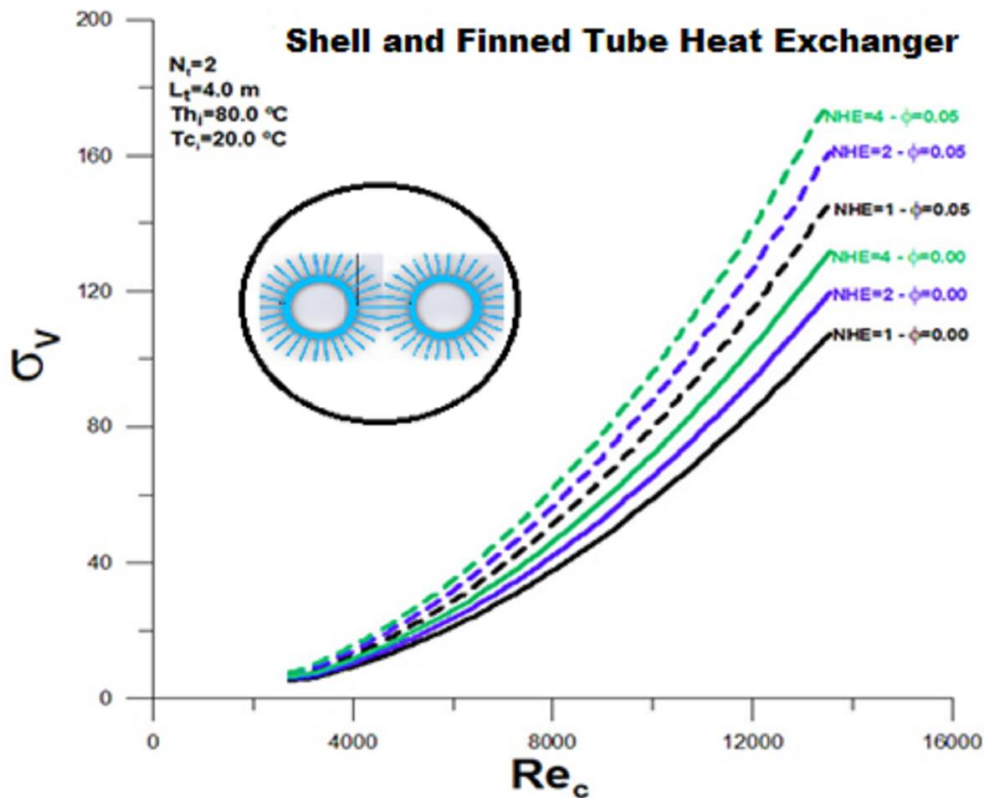


Figure 15. Viscous irreversibility for number of finned tubes equal to 2.

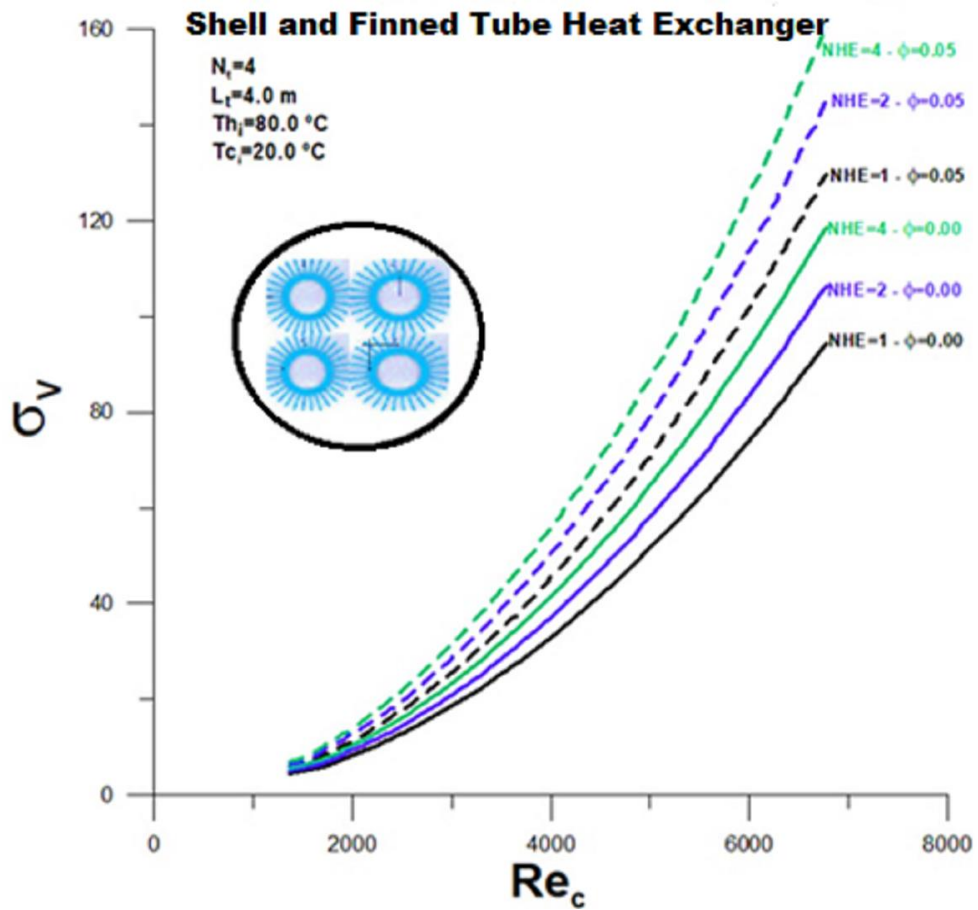


Figure 16. Viscous irreversibility for number of finned tubes equal to 4.

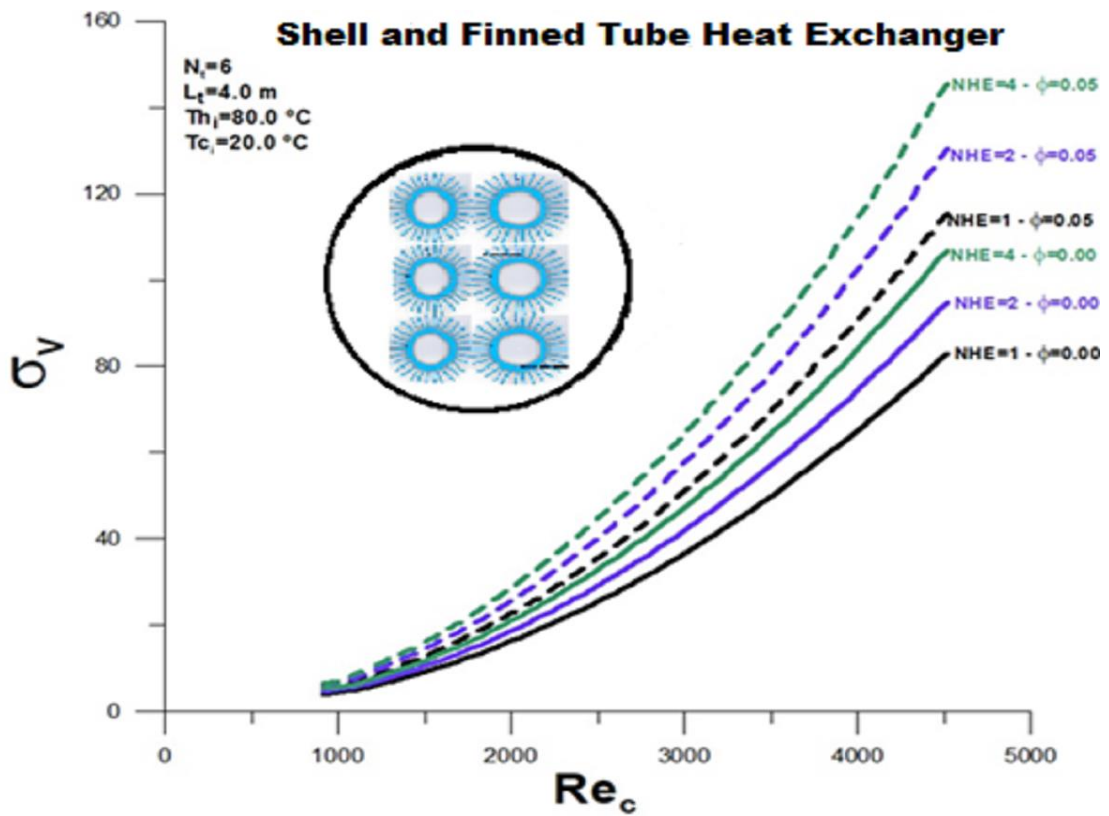


Figure 17. Viscous irreversibility for number of finned tubes equal to 6.

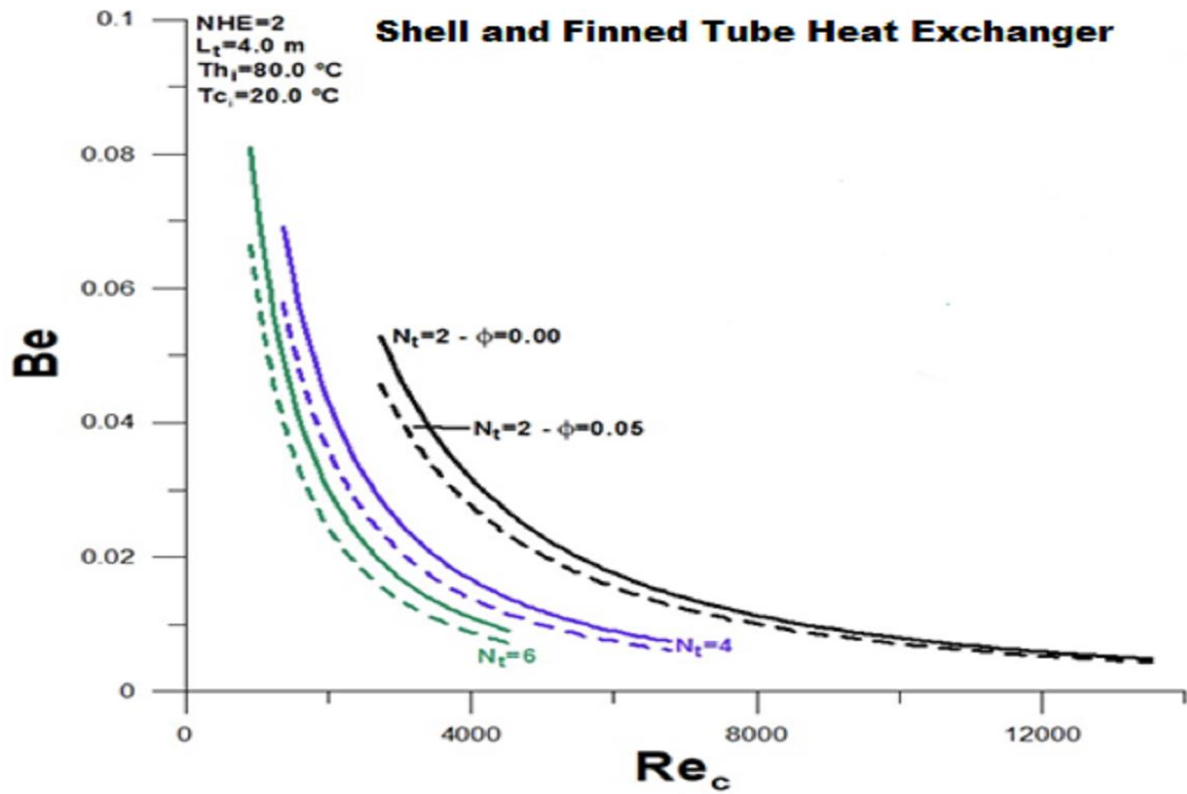


Figure 18. Thermodynamic Bejan number for number of heat exchangers equal to 2.

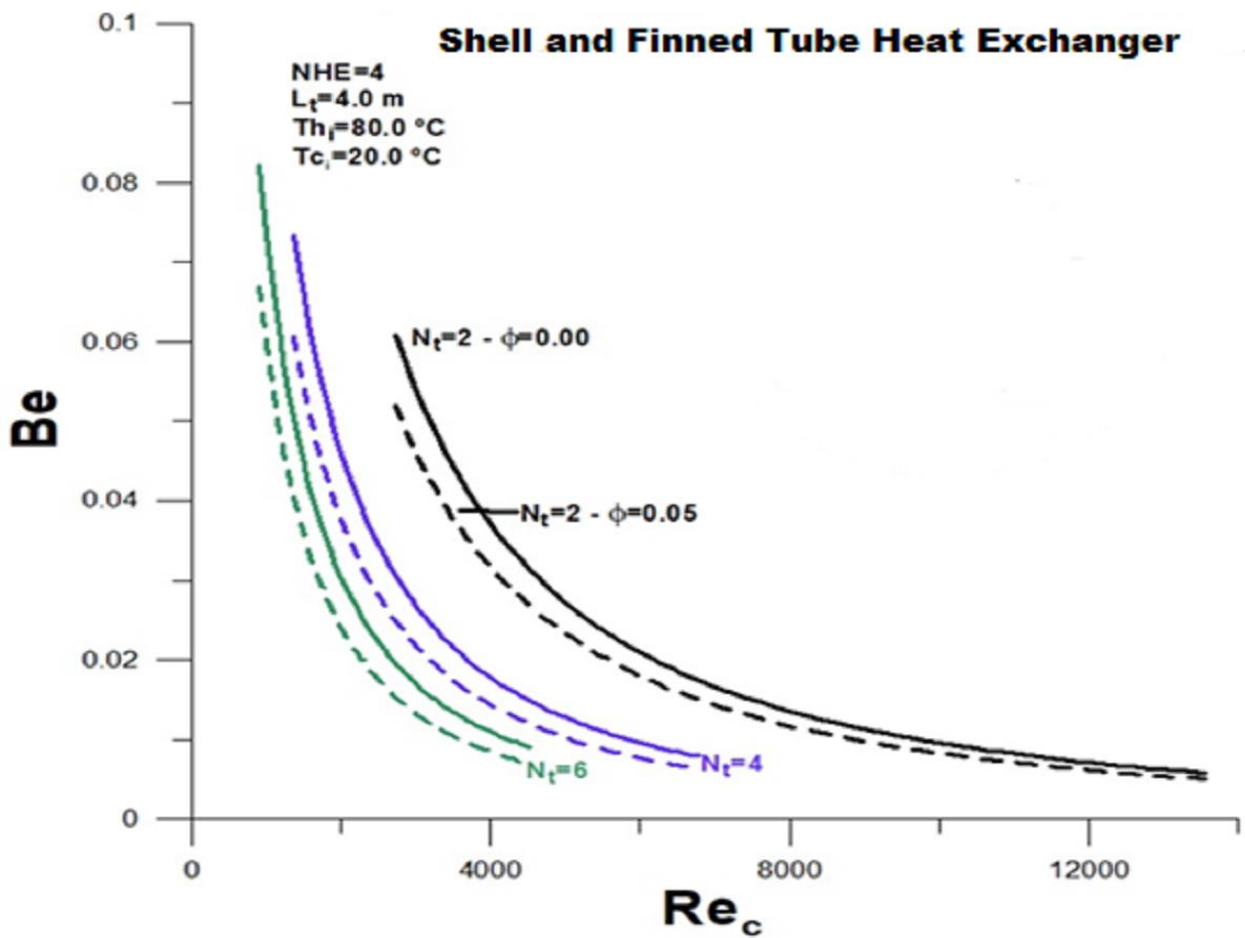


Figure 19. Thermodynamic Bejan number for number of heat exchangers equal to 4.

Figures 18 and 19 show the results obtained for the thermodynamic Bejan number for a few finned tubes equal to 2, 4, and 6, respectively. The Bejan number is the ratio between thermal irreversibility and total irreversibility (thermal + viscous). The values presented are significantly low, with great relevance to the viscous irreversibility. As already observed, more excellent performance can be marked with an increase in the number of finned tubes, with and without nanoparticles.

Since what leads to better thermal performance influences and contributes to more significant viscous loss, the need to cool the oil to a specific temperature is a price. However, it should be noted that the expansion of finned tubes can lead to cost-effectiveness improvement over time of use of the considered configuration.

The presented methodology makes it possible to increase the number of finned tubes and digits of heat exchangers automatically, paying attention to the internal diameter of the annular region, whose area must surpass the space occupied by the finned tubes. Therefore, the increase in the number of tubes is expected to improve the thermal performance versus viscous dissipation relationship.

4. CONCLUSIONS

The application refers to the cooling of machine oil flowing in the annular region, including non-spherical cylindrical nanoparticles of Boehmite Alumina. The main parameter in the optimization process is the number of finned tubes used for oil cooling. Another optimization factor is the number of heat exchanger units connected by hairpin.

The numbers show that the expansion of finned tubes brings a significant gain in thermal performance when added to the increase in the number of heat exchangers.

The thermal effectiveness reaches a maximum value approximately equal to 0.6 for two finned tubes and 0.9 for six finned tubes, within the flow range under analysis.

The pressure drop grows with the increase in heat exchangers and the inclusion of nanoparticles. However, it decreases significantly when the number of finned tubes is increased. This decrease is related to the relative increase in the area for oil flow and is highly relevant to the system's overall performance under analysis. Viscous irreversibility increases with the number of heat exchangers and decreases with the number of tubes.

Since what leads to better thermal performance influences and contributes to more significant viscous loss, the need to cool the oil to a specific temperature is a price. However, it should be noted that the expansion of finned tubes can lead to cost-effectiveness improvement over time of use of the considered configuration.

The increase in the number of finned tubes is expected further to improve the thermal performance versus viscous dissipation relationship.

Funding: This study received no specific financial support.

Competing Interests: The author declares that there are no conflicts of interests regarding the publication of this paper.

REFERENCES

- [1] I. Zafar, S. S. Khalid, and I. Muhammad, "Optimum configurations of annulus with triangular fins for laminar convection," *Thermal Science*, vol. 21, pp. 161-173, 2017.
- [2] I. Muhammad, K. S. Syed, Z. Iqbal, and A. Hassan, "A conjugate heat transfer analysis of a triangular finned annulus based on DG-FEM," *Mathematical Problems in Engineering*, pp. 1-18, 2018. Available at: <https://doi.org/10.1155/2018/6947565>.
- [3] A. Ghazala, K. S. Syed, and M. Ishaq, "Finite difference solution of conjugate heat transfer in double pipe with trapezoidal fins," *Numerical Modeling and Computer Simulation*, 2019. Available at: <https://doi.org/10.5772/intechopen.82555>.

- [4] I. Muhammad., A. Ali, M. Amjad, K. S. Syed, and Z. Iqbal, "Diamond-shaped extended fins for heat transfer enhancement in a double-pipe heat exchanger: An innovative design," *Applied Sciences*, vol. 11, pp. 1-21, 2021. Available at: <https://doi.org/10.3390/app11135954>.
- [5] R. G. Arvind and L. Yeshyahou, "A semi-empirical methodology for performance estimation of a double pipe finned heat exchanger," in *Proceedings of the 9th Biennial ASME Conference on Engineering Systems Design and Analysis, July 7-9, 2008, Haifa, Israel*, 2008.
- [6] G. Górecki, M. Łęcki, A. N. Gutkowski, D. Andrzejewski, B. Warwas, M. Kowalczyk, and A. Romaniak, "Experimental and numerical study of heat pipe heat exchanger with individually finned heat pipes," *Energies*, vol. 14, pp. 1-26, 2021. Available at: <https://doi.org/10.3390/en14175317>.
- [7] M. Prottay, R. J. Ishan, M. Sumit, and M. M. Ali, "Oil cooler: Finned-tube double-pipe heat exchanger." A ME 310 Project. Department of Mechanical Engineering Bangladesh University of Engineering and Technology. Supervisor: Dr. A. K. M. Monjur Morshed & Dr. Md. Ashiqur Rahman," 2020.
- [8] K. V. K. K. Shiva and K. Murthy, "Numerical study of heat transfer in a finned double pipe heat exchanger," *World Journal of Modelling and Simulation*, vol. 11, pp. 43-54, 2015.
- [9] M. Ayon, M. L. Khalid, T. Md Mahbub, and A. Md Younus, "Design of a shell and tube heat exchanger: Oil cooler for marine applications," Bangladesh University of Engineering & Technology Technical Report 2020.
- [10] S. Heidar, M. Aliehyaei, and M. A. Rosen, "Optimization of a finned shell and tube heat exchanger using a multi-objective optimization genetic algorithm," *Sustainability*, vol. 7, pp. 11679-11695, 2015.
- [11] A. Faraz, A. Sözen, A. Khanlari, and A. D. Tuncer, "Heat transfer enhancement of finned shell and tube heat exchanger using Fe₂O₃/water nanofluid," *Journal of Central South University*, vol. 28, pp. 3297-3309, 2021.
- [12] É. Nogueira, "Theoretical analysis of a shell and tubes condenser with r134a working refrigerant and water-based oxide of aluminum nanofluid (Al₂O₃)," *Journal of Materials Science and Chemical Engineering*, vol. 8, pp. 1-22, 2020.
- [13] E. Nogueira, "Thermal performance in heat exchangers by the irreversibility, effectiveness, and efficiency concepts using nanofluids," *Journal of Engineering Sciences*, vol. 7, pp. F1-F7, 2020.
- [14] M. Monfared, A. Shahsavar, and M. R. Bahrebar, "Second law analysis of turbulent convection flow of boehmite alumina nanofluid inside a double-pipe heat exchanger considering various shapes for nanoparticle," *Journal of Thermal Analysis and Calorimetry*, vol. 135, pp. 1521-1532, 2019.
- [15] A. Fakheri, "Heat exchanger efficiency," *Transactions of the ASME*, vol. 129, pp. 1268- 1276, 2007.
- [16] A. Bejan, "The thermodynamic design of heat and mass transfer processes and devices," *International Journal of Heat and Fluid Flow*, vol. 8, pp. 258-276, 1987.

Views and opinions expressed in this article are the views and opinions of the author(s), International Journal of Chemical and Process Engineering Research shall not be responsible or answerable for any loss, damage or liability etc. caused in relation to/arising out of the use of the content.